Carcinogenesis vol.33 no.4 pp.859–867, 2012
doi:10.1093/carcin/bgs024
Advance Access publication January 27, 2012

Opposing effects of bortezomib-induced nuclear factor-κB inhibition on chemical lung carcinogenesis

Sophia P.Karabela[1], Ioannis Psallidas[1,2], Taylor P.Sherrill[3], Chrysoula A.Kairi[1], Rinat Zaynagetdinov[3], Dong-Sheng Cheng[3], Spyridoula Vassiliou[4], Frank McMahon[3], Linda A.Gleaves[3], Wei Han[3], Ioannis Stathopoulos[1,5], Spyros G.Zakynthinos[1], Fiona E.Yull[3,6], Charis Roussos[1], Ioannis Kalomenidis[1,2], Timothy S.Blackwell[3,6,7,8] and Georgios T.Stathopoulos[1,3,5,*]

[1]Applied Biomedical Research and Training Center 'Marianthi Simou', Department of Critical Care and Pulmonary Services, General Hospital 'Evangelismos', School of Medicine, National and Kapodistrian University of Athens, 10675 Athens, Greece, [2]2nd Department of Pulmonary Medicine, University Hospital ''Attikon'', School of Medicine, National and Kapodistrian University of Athens, 12462 Haidari, Greece, [3]Department of Medicine, Division of Allergy, Pulmonary and Critical Care Medicine, Vanderbilt University School of Medicine, Nashville, TN 37232, USA, [4]Department of Hematology and Lymphomas, General Hospital 'Evangelismos', 10675 Athens, Greece, [5]Laboratory for Molecular Respiratory Carcinogenesis, Department of Physiology, Faculty of Medicine, University of Patras, 26504 Rio, Greece, [6]Department of Cancer Biology, [7]Department of Cell and Developmental Biology, Vanderbilt University School of Medicine, Nashville, TN 37232, USA and [8]Department of Veterans Affairs Medical Center, Tennessee Valley Healthcare System, Nashville, TN 37212-2637, USA

*To whom correspondence should be addressed. Department of Physiology, Faculty of Medicine, University of Patras, Basic Biomedical Sciences Research Building, 2nd floor, Room B40, 1 Asklepiou Street, University Campus (Panepistimioupolis), 26504 Rio, Greece. Tel: +30 2610 969155; Fax: +30 2610 997215;
Email: gstathop@upatras.gr

Since recent evidence indicates a requirement for epithelial nuclear factor (NF)-κB signaling in lung tumorigenesis, we investigated the impact of the NF-κB inhibitor bortezomib on lung tumor promotion and growth. We used an experimental model in which wild-type mice or mice expressing an NF-κB reporter received intraperitoneal urethane (1 g/kg) followed by twice weekly bortezomib (1 mg/kg) during distinct periods of tumor initiation/progression. Mice were serially assessed for lung NF-κB activation, inflammation and carcinogenesis. Short-term proteasome inhibition with bortezomib did not impact tumor formation but retarded the growth of established lung tumors in mice via effects on cell proliferation. In contrast, long-term treatment with bortezomib resulted in significantly increased lung tumor number and size. This tumor-promoting effect of prolonged bortezomib treatment was associated with perpetuation of urethane-induced inflammation and chronic upregulation of interleukin-1β and proinflammatory C-X-C motif chemokine ligands (CXCL) 1 and 2 in the lungs. In addition to airway epithelium, bortezomib inhibited NF-κB in pulmonary macrophages *in vivo*, presenting a possible mechanism of tumor amplification. In this regard, RAW264.7 macrophages exposed to bortezomib showed increased expression of interleukin-1β, CXCL1 and CXCL2. In conclusion, although short-term bortezomib may exert some beneficial effects, prolonged NF-κB inhibition accelerates chemical lung carcinogenesis by perpetuating carcinogen-induced inflammation. Inhibition of NF-κB in pulmonary macrophages appears to play an important role in this adverse process.

Abbreviations: BAL, bronchoalveolar lavage; CCL, C-C motif chemokine ligand; COPD, chronic obstructive pulmonary; CXCL, C-X-C motif chemokine ligand; GFP, green fluorescent protein; LLC, Lewis lung carcinoma; NF, nuclear factor; NSCLC, non-small cell lung cancer; PCNA, proliferating cell nuclear antigen; TNF, tumor necrosis factor; TUNEL, Terminal Deoxynucleotidyl Transferase-Mediated dUTP Nick End Labeling.

Introduction

Lung cancer presents a contemporary epidemic causing more deaths than the next three leading cancers combined (1,2). Of its different histologic subtypes, non-small cell lung cancer (NSCLC) including adenocarcinoma constitutes the bulk of new disease and is rising in incidence (3). Although most lung cancers are caused by smoking, the preponderance of new cases is diagnosed in ex-smokers (4,5). In addition, many lung cancers occur in never-smokers (6,7), and chronic inflammatory lung conditions such as chronic obstructive pulmonary disease (COPD) appear to promote carcinogenesis independent from smoking (3,8,9). Thus, although smoking cessation is fundamental for lung cancer prevention, additional strategies for early detection and prevention are needed, necessitating a better understanding of the molecular pathways that promote carcinogenesis in the human airways (10,11).

In recent years, proinflammatory NF-κB signaling has emerged as an important pathway to lung adenocarcinoma. We have shown that airway epithelial NF-κB activation is necessary for lung carcinogenesis induced by the carcinogen urethane (12). NF-κB is also required for lung adenocarcinoma formation in response to tobacco smoke and oncogenic *Kras* (13,14). We further identified respiratory epithelial NF-κB to function as a direct promoter of inflammation and carcinogenesis, implying NF-κB as a focal path to both lung cancer and COPD (15). In our previous studies, urethane-induced NF-κB activation was confined to lung epithelium and macrophages; importantly, tissue-specific blockade of epithelial NF-κB reduced lung tumors by greater than 2-fold (12). Although these studies suggest that NF-κB activation in both epithelial and inflammatory cells impacts lung tumor development, limited efforts have been undertaken to pharmacologically block NF-κB in preclinical lung cancer models.

Since NF-κB functions as a marked tumor promoter, drug-based approaches to inhibit NF-κB have been developed (16). These include direct blockade of inhibitor of NF-κB (IκB) kinase (IKK) β, the main NF-κB activator (17), as well as proteasome inhibition, which indirectly blocks NF-κB by suppressing IκB degradation (18). Although less specific, the latter approach has been tested more extensively. Bortezomib is clinically used against multiple myeloma and blocks NF-κB in a variety of tumors (19–21). In the lungs, NF-κB is activated in NSCLC and preneoplastic lesions (22), and bortezomib potently inhibits NF-κB in mouse lung adenocarcinoma (23), setting a rational framework for the use of the proteasome inhibitor in early stages of lung cancer. In humans, bortezomib has thus far failed to exhibit significant clinical activity against human NSCLC (24,25). To date, the mechanism(s) underlying human NSCLC resistance to bortezomib are unknown.

We aimed to investigate the effects of proteasome inhibition on chemical lung carcinogenesis, utilizing an established mouse model where a chemical carcinogen drives epithelial NF-κB activation, inflammation and carcinogenesis. Although we hypothesized that bortezomib would halt urethane-induced lung tumorigenesis, we found that the drug exerts both beneficial and detrimental effects, which are dependent on treatment timing and duration and are possibly linked with cell type-specific effects of bortezomib-mediated NF-κB blockade.

Materials and methods

Reagents

Urethane (ethyl carbamate) was from Sigma (St Louis, MO); bortezomib (Janssen-Cillag Hellas, Athens, Greece) was from the pharmacy; D-luciferin was from Biosynth AG (Naperville, IL); MTS assay was from Promega (Madison, WI); anti-proliferating cell nuclear antigen (PCNA) antibody from Santa Cruz (Santa Cruz, CA); Terminal Deoxynucleotidyl Transferase-Mediated dUTP Nick End Labeling (TUNEL) from Roche (Penzberg, Germany); mouse tumor necrosis factor (TNF), C-C motif chemokine ligand (CCL) 2 (monocyte

chemoattractant protein-1, MCP-1), C-X-C motif chemokine ligand (CXCL) 1 (keratinocyte chemoattractant, KC), CXCL2 (macrophage inflammatory protein 2, MIP-2) and interleukin (IL)-1β enzyme-linked immunosorbent assays from R&D Systems (Minneapolis, MN) and Peprotech (London, UK) (detection limits: 1.5, 5.1, 15.6, 7.8, 1.5 and 7.8 pg/ml, respectively) and mouse cytometric bead array assaying TNF, IFN-γ, CCL2, IL-6, IL-10 and IL-12p70 from BD Biosciences (San Jose, CA) (detection limits: 7.3, 2.5, 52.7, 5.0, 17.5 and 10.7 pg/ml, respectively).

Microscopy

Stereomicroscopy of gross mouse lung specimens with urethane-induced tumors was done on a StemiDV4 stereomicroscope connected to a handheld digital camera (Zeiss, Jena, Germany). Light microscopy was performed on an IX71 inverted microscope connected to a DP digital camera (Olympus, Tokyo, Japan). Fluorescent microscopy was performed on an IX81 inverted microscope with spinning disc confocal configuration connected to a CAM-XC50 cooled digital color camera (Olympus, Tokyo, Japan), using Image-Pro Express software (Media Cybernetics, Silver Springs, MD).

Animals

In total, 177 mice were used for these studies. Wild-type BALB/c and FVB mice from the Hellenic Pasteur Institute (Athens, Greece) were inbred at the Animal Care facilities of the General Hospital Evangelismos (Athens, Greece). Dual luciferase-green fluorescent protein (GFP) NF-κB reporter (NF-κB.GFP. Luciferase, NGL) mice (>F12 FVB background) (12,15,26) were bred and used at the Animal Care facilities of Vanderbilt University (Nashville, TN). Animal care and experimental procedures were approved by the Prefecture of Athens Veterinary Administration Bureau (Greece) or the Vanderbilt University Institutional Animal Care and Use Committee and conducted according to international standards (http://grants.nih.gov/grants/olaw/GuideBook.pdf; http://ec.europa.eu/environment/chemicals/lab_animals/legislation_en.htm). Experimental mice were sex, weight (20–24 g) and age (8–10 weeks) matched.

Carcinogen and drug treatments

For induction of lung tumors, mice received single or four weekly intraperitoneal (i.p.) injections of urethane (1 g/kg in 100 μl saline), as indicated. Bortezomib (1 mg/kg in 100 μl saline i.p.) was administered during distinct time windows of tumor initiation/promotion, tumor progression or both (month 1, month 5 or continuously after the first urethane injection) at days 2 and 5 of each experimental week. All mice not treated with urethane or bortezomib at a given time point received saline instead (100 μl i.p.). Mice were killed at days 7, 10, 30, 60 or 180 after the first urethane dose, as indicated.

Assessment of lung inflammation

Bronchoalveolar lavage (BAL) was performed with 3 × 1000 μl sterile saline. Fluid was combined and centrifuged (260*g*, 10 min), cells were resuspended in 1 ml phosphate-buffered saline and 1% bovine serum albumin, total cell counts were determined using a grid hemocytometer and differential cell counts by enumerating 400 cells on Wright-Giemsa-stained cytocentrifugal specimens. Levels of solute mediators in cell-free BAL were determined by cytometric bead array (TNF, IFN-γ, CCL2, IL-6, IL-10, IL-12p70) and/or enzyme-linked immunosorbent assay (TNF, CCL2, CXCL1, CXCL2, IL-1β) as described previously (12,23) and were corrected for BAL protein assessed using bovine serum albumin assay (Bio-Rad, Hercules, CA).

Assessment of lung carcinogenesis

Lungs were explanted after transtracheal inflation with 10% neutral buffered formalin under 25 cm H_2O pressure and fixed in the same solution for 24 h. Lung tumors were enumerated by three blinded readers (S.P.K., I.P., G.T.S.) under a stereomicroscope using surface- and transillumination to visualize both superficial and intrapulmonary tumors and averaged as described previously (12,15). Tumor diameter (δ) was determined using microcalipers, and tumor volume (V) was determined using the formula $V = \pi\delta^3/6$. Total tumor burden for each mouse was calculated by adding the volumes of all tumors from the lungs of each mouse. Lungs were embedded in paraffin in a standard fashion and 5 μm thick serial transverse sections were cut at three levels of the lungs (apical, median and basal). Sections were mounted on glass slides and stained with hematoxylin and eosin. The total number and the proportion (percent of total lung lesions) of each type of distinct lung lesions, including hyperplasia (atypical alveolar or bronchial epithelial hyperplasia), adenoma and adenocarcinoma, were evaluated by two blinded readers (S.P.K. and G.T.S.) on three sections from each lung (one apical, one median and one basal transverse section of both lungs), according to guidelines of the Mouse Models of Human Cancers Consortium (27). Alternatively, sections were immune labeled for PCNA and TUNEL as described previously (12,15,28). The number of immunoreactive cells in lungs (bronchial and alveolar epithelium) and lung tumors was evaluated by two blinded readers (S.P.K. and G.T.S.) in five high-power visual fields of five different lung or tumor regions. The results were averaged per mouse.

Assessment of pulmonary NF-κB activation

NGL mice received intravenously 1 mg D-luciferin and were imaged for bioluminescence at days 0, 3, 7 and 10 after saline or urethane, as described previously (12,15,26,29,30). At day 10, lungs were explanted immediately imaged for bioluminescence *ex vivo*, fixed, embedded and sectioned as above. Sections were mounted on glass slides using aqueous low-fluorescence mounting medium containing 4,6-diamidino-2-phenylindole (30). GFP expression of lung components was evaluated in 10 high-power visual fields of each lung tested.

Cell culture experiments

Mouse Lewis lung carcinoma (LLC) cells and bone marrow-derived macrophages (RAW264.7) validated by the short tandem repeat method were purchased from the American Type Culture Collection (ATCC, Manassas, VA) in July 2007 and were immediately frozen at −80°C . Cells were resuscitated in May 2009 and experiments were done within 6 months. Cell lines were cultured at 37°C in 5% CO_2–95% air using Dulbecco's modified Eagle's medium, 10% fetal bovine serum supplemented with glutamine and 100 mg/l penicillin/streptomycin. RAW264.7 cells were stably transduced with an NF-κB reporter plasmid (NF-κB.GFP.LUC; pNGL) as described previously (30,31). For cell experiments, cells were plated at equal densities and incubated with saline or various concentrations of bortezomib. Viable cell numbers were determined using MTS reduction (23,28–31). NF-κB activation was determined using both bioluminescence imaging and luciferase assay (23,28–30). Cellular mediator elaboration was assessed using cytometric bead array/enzyme-linked immunosorbent assay of cell-free cell culture supernatants and was corrected for protein content.

Subcutaneous tumor growth model

Solid adenocarcinomas were generated by flank injections of 5×10^5 wild-type or pNGL LLC cells in C57BL/6 mice (23). Three vertical tumor dimensions (δ1, δ2, δ3) were measured weekly and tumor volume (V) was determined using the formula $V = \pi \times (\delta1 \times \delta2 \times \delta3)/6$. Tumor-specific NF-κB activation was also measured weekly as described previously (23). Mice received twice weekly i.p. saline control or bortezomib (1 mg/kg) starting at 2 weeks post tumor cell injection.

Statistics

All values given represent mean ± SD. To compare variables between two groups, the Student's *t*-test or the Mann–Whitney *U*-test were used for normally and not normally distributed variables, respectively. To compare variables between multiple groups, one-way analysis of variance with Tukey's *post hoc* tests or Kruskal–Walis test with Dunn's *post hoc* tests were used for normally and not normally distributed variables, respectively. All *P*-values are two tailed. $P < 0.05$ was considered significant. Statistical analyses were performed using GraphPad Prism 5.0 (San Diego, CA).

Results

Short-term bortezomib treatment does not impact urethane-induced lung tumor initiation but significantly retards established tumor growth. In contrast, prolonged proteasome inhibition promotes the formation and progression of lung tumors

For these experiments, 63 BALB/c mice received four weekly urethane injections. Twice weekly drug treatment was started immediately after the first urethane dose in four different protocols: control mice received twice weekly saline for 6 months, mice enrolled in an initiation/promotion trial received bortezomib during the first month and saline thereafter, mice enrolled in a regression trial received bortezomib during the fifth month and saline before and thereafter and mice enrolled in a prolonged prevention trial received bortezomib continuously for 6 months (Figure 1A). Out of 15, 16, 17 and 15 mice enrolled in the control, initiation/promotion, regression and prolonged prevention protocols, 2, 5, 2 and 4, respectively, succumbed prematurely (log-rank $P = 0.462$; $\chi^2 = 0.475$) and one animal each from the regression and prolonged prevention protocols developed massive ($\delta > 1$ cm) thyroid tumors that required euthanasia (images not shown), leaving 13, 11, 14 and 10 mice from the four protocols for analyses. Compared with controls (mean lung tumor number = 6.6 ± 2.9 and diameter = 1.03 ± 0.27 mm), mice in the initiation/promotion trial developed lung tumors of similar multiplicity (6.5 ± 3.9; $P = 0.949$) and

size (mean diameter = 0.96 ± 0.20 mm; $P = 0.351$) (Figure 1B and C). Histologic distribution of lesions (hyperplasia, adenoma and adenocarcinoma) was identical between groups (data not shown). In the regression trial, a similar number of lung tumors (7.5 ± 4.3; $P = 0.494$) was identified in bortezomib-treated mice compared with the control group; however, tumors were significantly reduced in size (mean diameter = 0.80 ± 0.12 mm; $P = 0.003$), resulting in a ~50% reduction in individual tumor volume and a ~60% decrease in total lung tumor burden per mouse (Figure 1B and C). Again, tumor histologic distribution was comparable with controls (data not shown). These results indicated that short-term proteasome inhibition does not impact the formation of new lung tumors by urethane (initiation/promotion) but exerts inhibitory effects on the growth of existing lung tumors.

In contrast to our expectations, mice that received bortezomib continuously (prolonged prevention trial) exhibited significantly increased lung tumor numbers (16.9 ± 3.4; $P < 0.001$) and diameters (1.36 ± 0.17 mm; $P < 0.001$) compared with control mice (Figure 1B and C), without changes in tumor histologic distribution (data not shown). These changes corresponded to a ~70% increase in individual tumor volume and a ~250% increase in total lung tumor burden per mouse. These findings indicated a marked chemical carcinogenesis-promoting effect of prolonged proteasome inhibition. Immunohistochemistry of lung tumors at the 6 months time point for PCNA and TUNEL staining, indicators of cell proliferation and apoptosis, respectively (14,16), yielded similar fractions of tumor cells displaying PCNA and TUNEL immunoreactivity among all experimental groups. Very few TUNEL positive cells were identified in any group (data not shown).

Based on previous work that showed a link between urethane-induced lung inflammation and carcinogenesis (12,15), we evaluated the inflammatory response in the airway compartment of the above experimental mice at the 6 months time point. Compared with controls, mice enrolled in the initiation/promotion and regression trials displayed similar levels of inflammatory cells and mediators in BAL. However, mice in the prolonged prevention group had markedly increased numbers of macrophages, lymphocytes and neutrophils, as well as significantly elevated levels of IL-6, CXCL1, CXCL2 and IL-1β in BAL (Figure 1E and F). These results suggested that the pro-tumorigenic effects of long-term bortezomib are linked with a persistent/dysregulated inflammatory response to urethane.

The oncogenic effect of prolonged bortezomib treatment is not strain specific

We next sought to recapitulate the effects of long-term proteasome inhibition using FVB mice, known for their susceptibility to

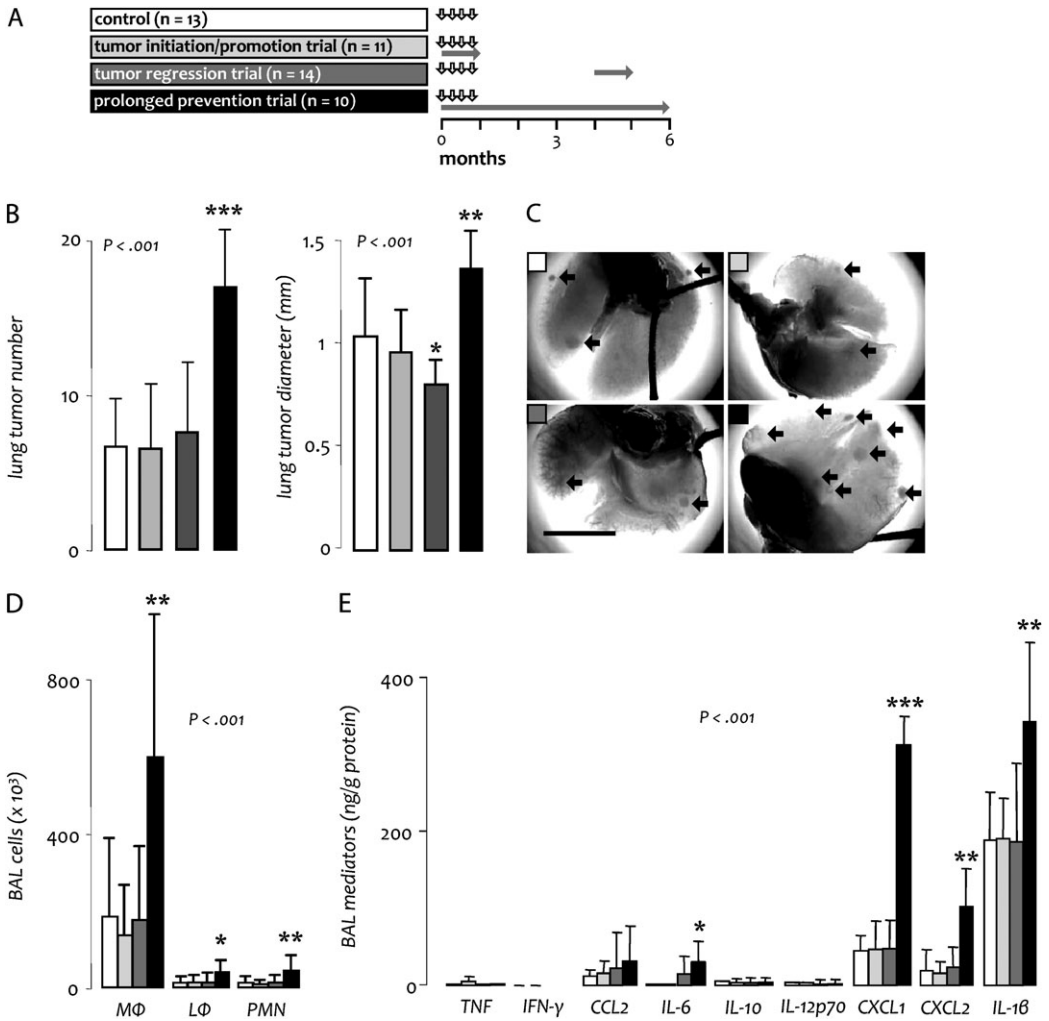

Fig. 1. Effects of proteasome inhibition on urethane-induced lung carcinogenesis in BALB/c mice. (**A**) Experimental setup of long-term studies in BALB/c mice. Vertical arrows indicate urethane treatment; horizontal gray arrows indicate periods of bortezomib treatment. (**B**) Tumor measurements at 6 months. (**C**) Representative photographs of tumor-bearing lungs (black arrows point to tumors; scale bar = 1 cm). (**D** and **E**) Inflammatory cells (D) and mediators (E) in BAL at 6 months. Columns, mean; bars, SD; *, ** and ***: $P < 0.05$, 0.01 and 0.001, respectively, compared with control; *n*, sample size; *P*, probability; MΦ, macrophages; LΦ, lymphocytes; PMN, neutrophil polymorphonuclear cells; IL, interleukin; TNF, tumor necrosis factor; IFN, interferon.

tumorigenesis (12). For this experiment, mice received a single dose of urethane, followed by twice weekly saline or bortezomib (Figure 2A). Compared with urethane-treated controls (mean lung tumor number = 5.2 ± 2.3 and diameter = 1.05 ± 0.31 mm), mice treated with bortezomib developed more (11.1 ± 1.4; $P = 0.001$) and larger (mean diameter = 1.35 ± 0.23 mm; $P = 0.048$) lung tumors (Figure 2B and C) after 4 months. Histologic tumor distribution was similar between groups (data not shown). These findings corresponded to an 80% increase in individual tumor volume and to a 280% increase in lung tumor burden per mouse in the bortezomib-treated group, indicating that the oncogenic effect of prolonged bortezomib is not mouse strain specific.

Continued bortezomib treatment promotes epithelial survival after urethane

To better understand the dichotomous effects of bortezomib treatment, we investigated early phases of urethane-induced lung inflammation and oncogenesis (15). For this, BALB/c mice received a single injection of saline or urethane followed by twice weekly saline or bortezomib for up to 1 month. Mice were terminated at days 7, 30 or 60 post urethane (Figure 3A). No histologic abnormalities were found at day 7 irrespective of treatment. At day 30, saline only-treated mice also had no hyperplastic lesions; however, a few foci of atypical adenomatous hyperplasia were detected in the lungs of urethane-treated mice (Figure 3B). Importantly, bortezomib treatment caused a significant increase in the number of these atypical adenomatous hyperplasia lesions, as well as evidence of cellular proliferation within them at day 30 (Figure 3C and D). Cells within hyperplastic lesions did not exhibit TUNEL staining. However, TUNEL+ cells were present in the remaining lung parenchyma, and their relative abundance was reduced in the bronchial and alveolar epithelium of bortezomib-treated mice compared with controls (Figure 3E). To explain the absence of bortezomib's neoplasia-promoting effects in mice treated only during the first month after urethane (initiation/promotion trial), separate groups of mice were examined at day 60, after bortezomib was withdrawn for 1 month (Figure 3A). At this time point, no differences in hyperplastic lesion abundance, cell proliferation or cell apoptosis were identified between experimental groups (data not shown), indicating that bortezomib-enhanced formation of premalignant hyperplasia lesions was reversible.

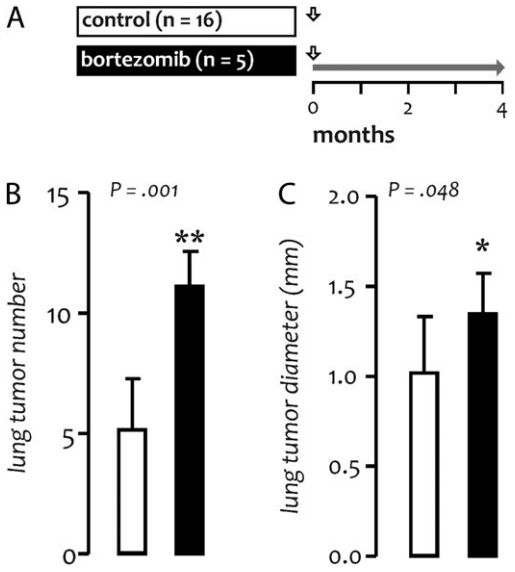

Fig. 2. Oncogenicity of prolonged bortezomib treatment in FVB mice. (**A**) Experimental setup of long-term studies in FVB mice. Vertical arrows indicate urethane treatment; horizontal gray arrow indicates period of bortezomib treatment. Tumor number (**B**) and diameter (**C**) at 4 months. Columns, mean; bars, SD; * and **: $P < 0.05$ and 0.01, respectively, compared with control; *n*, sample size; *P*, probability.

Bortezomib treatment perpetuates urethane-induced lung inflammation despite blocking NF-κB in epithelium and macrophages

To better understand the impact of bortezomib on the evolution of urethane-induced inflammation in the lungs, we analyzed inflammatory cells and mediators in BAL from mice harvested at 7 and 30 days after urethane (Figure 3A). At experimental day 7, when urethane-induced inflammation peaks (12,15), urethane-treated mice had increased numbers of inflammatory cells, including macrophages, lymphocytes and neutrophils, as well as inflammatory mediators in BAL, including TNF, CCL2, CXCL1 and CXCL2, compared with controls. At this time point, bortezomib treatment caused significant reductions in most of these parameters. Interestingly, bortezomib-treated mice had elevated concentration of IL-6 in BAL, a finding not present in the other groups (Figure 3F and G). At experimental day 30, a time point when urethane-induced inflammation should subside (12,15), urethane-treated mice and saline-treated controls showed no evidence of inflammation. In marked contrast, bortezomib-treated mice exhibited significantly increased BAL macrophage, lymphocyte and neutrophil numbers, as well as elevated CXCL1, CXCL2 and IL-1β levels compared with mice treated only with urethane. In addition, these mice continued to have increased IL-6 concentration in BAL (Figure 3H and I). Collectively, these results suggested that systemic proteasome inhibition of urethane-exposed mice partially inhibits the acute lung inflammatory response to the carcinogen, but continued proteasome inhibition results in perpetuation of this inflammatory response with chronic upregulation of chemokine and interleukin expression.

To verify that bortezomib treatment blocks urethane-induced NF-κB activation and to investigate the lung cell types affected by this treatment, we utilized NF-κB reporter (NGL) mice (FVB background) that express a GFP-luciferase fusion protein under control of an NF-κB-dependent promoter (26). NGL mice received urethane followed by twice weekly bortezomib or saline, were serially imaged for bioluminescence and were killed after 10 days (Figure 4A). We found that the proteasome inhibitor blocked overall urethane-induced NF-κB activation in the lungs (Figure 4B and C). At the tissue level, NF-κB inhibition by bortezomib was not confined to airway epithelium but was also observed in alveolar macrophages *in vivo* (Figure 4D and E).

Short-term bortezomib can limit the growth of established lung adenocarcinoma

To verify the beneficial impact of bortezomib on the progression of already formed lung tumors, we generated heterotopic tumors induced by wild-type LLC lung adenocarcinoma in the flank of syngeneic C57BL/6 mice and installed twice weekly bortezomib or control treatments starting after 2 weeks (Figure 5A). Short-term bortezomib at 1 mg/kg was able to retard flank LLC tumor growth, an effect associated with reduced tumor cell proliferation (Figure 5B and C). Repetition of this experiment using pNGL LLC cells (23,28–31) verified that this inhibitory impact of bortezomib was associated with reduced NF-κB activity in tumor cells (Figure 5D and E). These results indicated that limited courses of bortezomib can favorably impact the growth of established lung adenocarcinoma by downregulating NF-κB activation and were consistent with the reduced tumor size observed after late bortezomib treatment (regression trial) in the urethane model.

Bortezomib alters the phenotype of RAW264.7 macrophages

Because deletion of IκB kinase (IKK) β has been shown to result in a paradoxical increase in IL-1β production in macrophages (32), we wondered whether prolonged pharmacological inhibition of NF-κB could result in increased cytokine/chemokine production by these cells. Therefore, we investigated the impact of proteasome inhibition on RAW264.7 macrophages *in vitro*. As expected, bortezomib treatment caused a dose-dependent suppression of proliferation and NF-κB

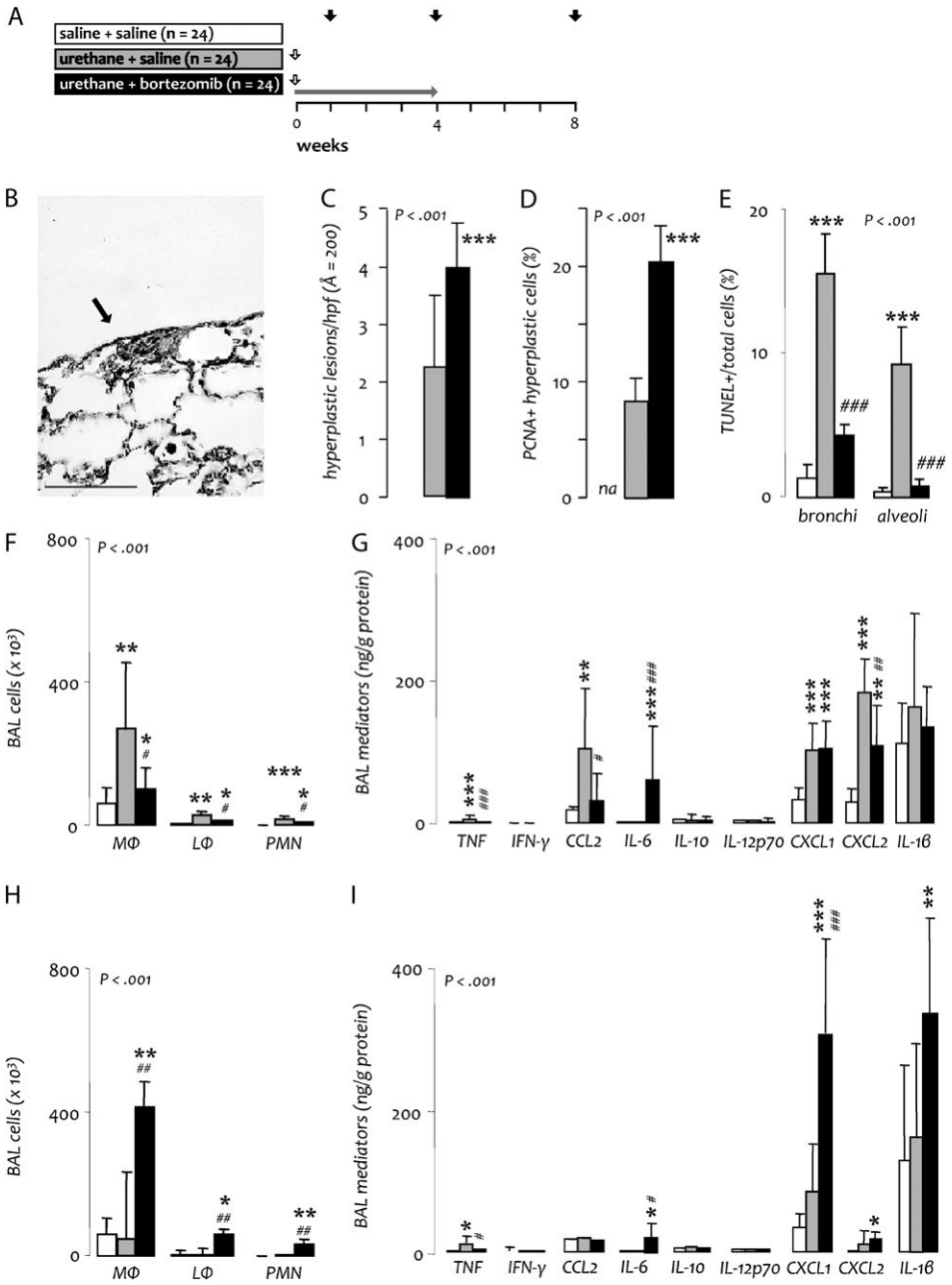

Fig. 3. Impact of bortezomib on early stages of urethane-induced lung inflammation and oncogenesis. (**A**) Experimental setup of short-term studies in BALB/c mice. Vertical white arrows indicate urethane treatment; horizontal gray arrow indicates period of bortezomib treatment; black arrows indicate mouse termination time points. (**B**) Representative atypical adenomatous hyperplasia of the lungs at 1 month (Å = 400; scale bar = 50 μm). (**C**) Cumulative number of hyperplastic lesions on three lung sections per mouse (apical, median and basal transverse). (**D**) Percentage of hyperplastic cells positive for PCNA. (**E**) Percentage of lung cells positive for TUNEL. (**F–I**) Inflammatory cells (F, H) and mediators (G, I) in BAL at day 7 (F, G) and 30 (H, I) post urethane. Columns, mean; bars, SD; *, ** and ***: $P < 0.05$, 0.01 and 0.001, respectively, compared with sham-treated mice (saline + saline); #, ## and ###: $P < 0.05$, 0.01 and 0.001, respectively, compared with urethane only-treated mice (urethane + saline); *n*, sample size; *P*, probability; MΦ, macrophages; LΦ, lymphocytes; PMN, neutrophil polymorphonuclear cells; IL, interleukin; TNF, tumor necrosis factor; IFN, interferon.

activation in these cells (Figure 6A and B). In addition, 48 h of exposure to the drug sufficed to alter RAW264.7 phenotype, including upregulation of CXCL1, CXCL2 and IL-1β secretion (Figure 6C). Interestingly, this shift in inflammatory mediator production mirrored the profile of cytokines/chemokines shown to be increased in the lungs of mice treated with the combination of urethane and prolonged bortezomib. This activation of bortezomib-treated RAW264.7 macrophages provides a plausible model for the effects of the proteasome inhibitor on lung macrophages *in vivo*, the altered function of which may underlie bortezomib-induced amplification of lung inflammation and tumorigenesis.

Discussion

We found that short-term treatment with bortezomib downregulates the initial inflammatory response to urethane but prevents resolution of urethane-induced inflammation. As a result, prolonged courses of treatment with the proteasome inhibitor were associated with enhanced lung carcinogenesis and a dysregulated persistent inflammatory response in the lungs. In contrast, bortezomib treatment retards the growth of established tumors, a finding consistent with prior reports (18,20,21,23). Interestingly, bortezomib treatment increased proliferation of cells within pulmonary hyperplastic lesions at 1 month

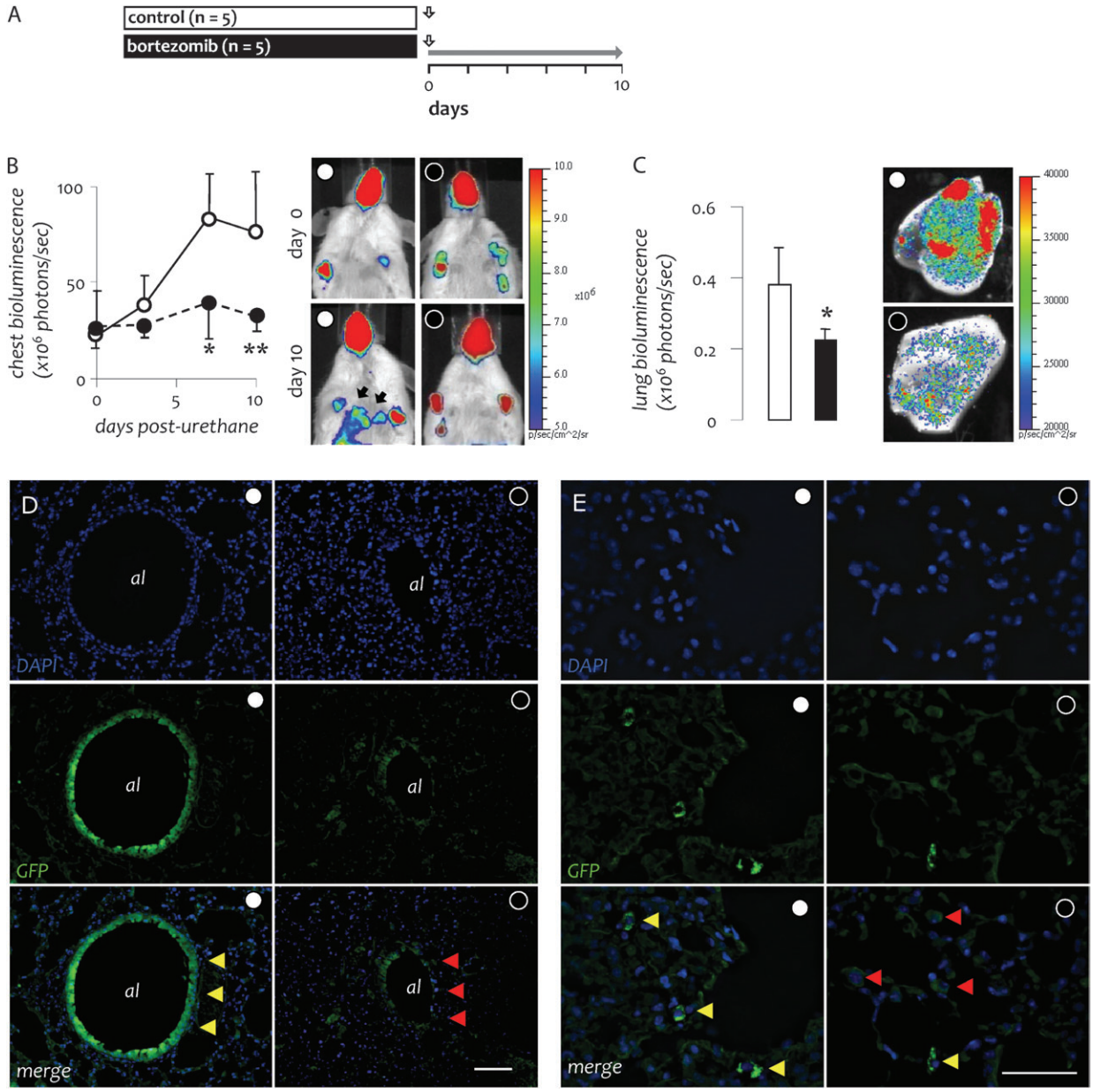

Fig. 4. Bortezomib inhibits urethane-induced NF-κB activation in both respiratory epithelium and pulmonary macrophages. (**A**) Experimental setup of NF-κB activation studies in transgenic NF-κB reporter mice expressing luciferase GFP under control of NF-κB (NGL; FVB strain). Vertical arrows indicate urethane treatment; horizontal gray arrow indicates period of bortezomib treatment. (**B**) Time course of chest photon emission as determined by *in vivo* bioluminescence imaging (left) and representative bioluminescent images (right). (**C**) Photon emission of lung explants at day 10 as determined by *ex vivo* bioluminescence imaging (left) and representative bioluminescent images (right). (**D**) Representative cross-sectioned airway epithelium (al = airway lumen) and (**E**) macrophages in pulmonary airspaces from urethane ± bortezomib-treated NGL mice. Blue and green fluorescence indicate, respectively, nuclear 4,6-diamidino-2-phenylindole staining and NF-κB-driven GFP expression. Yellow and red arrowheads indicate cells with high and low NF-κB activity, respectively. (D, Å = 100; scale bar = 200 μm; E, Å = 400; scale bar = 100 μm). Points in B and columns in C, mean; bars, SD. * and **: $P < 0.05$ and 0.01, respectively, compared with saline-treated mice.

after urethane injection in association with increased levels of inflammatory cells and mediators in the lungs. However, proliferation of cells in established heterotopic LLC tumors was reduced by bortezomib treatment. This finding, combined with data indicating that bortezomib enhances inflammatory mediator production by myeloid cells, suggests that the opposing effects of NF-κB inhibition may depend on the impact of this treatment on inflammatory cells in the tumor microenvironment. In the setting of carcinogens like urethane, which promote tumor formation through activation of inflammatory pathways, inhibition of NF-κB in myeloid cells may prevent resolution of inflammation, enhancing the pro-tumorigenic microenvironment. In contrast, beginning bortezomib treatment after carcinogen-induced inflammation has subsided (as in the regression trial) or in models where inflammation is not driven by carcinogen exposure (like the heterotopic LLC tumor model) appears to reduce tumor growth through tumor-specific effects of NF-κB inhibition on cell proliferation. These findings may have important implications for chemotherapeutic approaches in individuals at high risk for lung cancer development, especially those with COPD, where chronic airway inflammation is a manifestation of the disease.

NF-κB, a central transcriptional pathway controlling immune responses, is increasingly identified as an important factor in a number of malignancies, including lung cancer (16). NF-κB is activated in biopsies from NSCLC and associated preneoplastic lesions (22). In addition, NF-κB activation has been identified in epithelial and myeloid cells in the lungs of COPD patients, the group of current and former

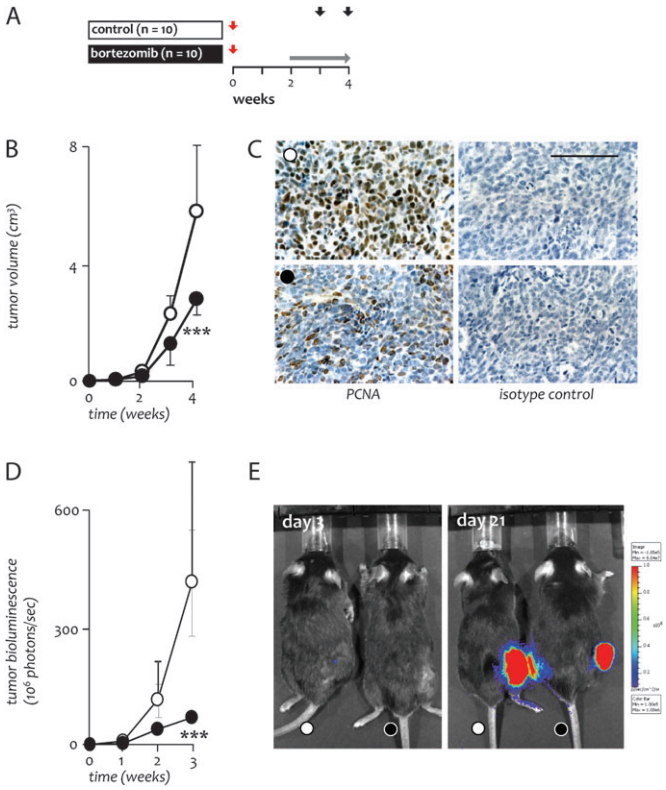

Fig. 5. Effects of bortezomib growth and NF-κB activity of established lung adenocarcinoma. (**A**) Experimental setup of tumor growth studies in C57BL/6 mice. Red arrows indicate LLC implantation; horizontal gray arrow indicates period of bortezomib treatment; black arrows indicate mouse termination time points. Mice received either wild-type or NF-κB reporter LLC cells. (**B**) Tumor volume ($n = 5$ per group). (**C**) Representative microphotographs of immunoreactivity of flank tumors for PCNA (left panels) and respective isotype controls (right panels) at 4 weeks (Å = 400; scale bar = 100 μm) (**D**) Tumor-restricted NF-κB activity ($n = 5$ per group). (**E**) Representative bioluminescence images at 3 and 21 days post-LLC transplant with pseudocolor scale bar; colored areas emit light stemming exclusively from tumor cells. Circles, mean; bars, SD. $^{***}P < 0.001$ compared with saline-treated mice.

smokers at highest risk for lung cancer development (33,34). Using functional studies of mice, we and others have shown that the transcription factor is activated in the lungs in response to tobacco and urethane (12,14). Moreover, several studies have shown that epithelial NF-κB activation is not only involved in carcinogen-induced lung inflammation but is required for adenocarcinoma formation and may promote tumor invasion and metastasis (12–14,35). Thus, the NF-κB pathway appears to be a promising drug target for lung cancer chemoprevention and treatment. Based on this idea, we performed systemic proteasome inhibition in mice during various time windows after carcinogen exposure, aiming to inhibit NF-κB activation and the associated inflammatory and oncogenic response. We found a tumor growth-inhibitory effect when bortezomib was administered for short periods of time in mice with established lung tumors. Our findings are consistent with a recent report by Xue *et al.* (36) in which treatment with bortezomib or an IκB kinase (IKK) inhibitor (Bay-117082) induced tumor regression and prolonged survival in mice expressing mutant Kras along with p53 deficiency. In this study, cells and tumors with the combination of mutant Kras expression and p53 deficiency, which have a high basal NF-κB activation, were more sensitive to bortezomib than cells and tumors with mutant Kras expression and intact p53, which have lower basal NF-κB activation, indicating a correlation between tumor cell NF-κB activation and response to bortezomib therapy. This correlation between NF-κB activation in tumor cells and treatment response is similar to clinical data in which the presence of an NF-κB signature in multiple myeloma is associated with a better outcome after bortezomib treatment (37).

In contrast to the beneficial effects of NF-κB inhibition during short periods of time in established tumors, prolonged treatment with bortezomib resulted in an unexpected and profound pro-tumorigenic effect. These results may be relevant to understand the outcome of clinical trials of bortezomib against NSCLC, which revealed no or modest single-agent activity of the drug (24,25). In these clinical studies, bortezomib was administered for prolonged periods of time (up to 8 or even unlimited 21 day cycles). Although some responses were identified, progressive disease ensued almost uniformly. It is plausible that the few clinically significant responses to bortezomib may have been, at least in part, attributable to inhibition of tumor NF-κB activity. However, long-term delivery of the drug might have perpetuated tumor-related inflammation and augmented tumor progression in a majority of cases. A pulmonary proinflammatory effect of the drug is also suggested by a recent study describing the pulmonary toxicity of bortezomib in myeloma patients (38). It is also possible that tumor progression was related to development of bortezomib resistance by tumor cells, as has been proposed based on another recent study (36). Our results indicate that prolonged bortezomib treatment facilitates development of preneoplastic lesions and progression to malignancy through propagation of airway inflammation. This may be relevant to humans since bronchogenic neoplasia typically occurs in an inflammatory environment (39,40). Hence, our results may sound a note of caution when considering prolonged treatment with this drug or the application of other NF-κB blocking agents to cancer treatment or chemoprevention.

While bortezomib treatment inhibited NF-κB activity in lung epithelium and myeloid cells, urethane-induced inflammation failed to resolve. In cultured macrophages, continuous bortezomib-induced NF-κB blockade resulted in upregulation of CXCL1/2 chemokines and IL-1β, possibly explaining persistent inflammation in bortezomib-treated mice after exposure to urethane. The amazing similarities of bortezomib effects on the BAL inflammatory milieu with that on a liver-derived macrophage cell line (RAW264.7) lend support to the hypothesis that the effects of the drug on alveolar macrophages may underlie its impact on the pulmonary inflammatory and oncogenic response. Although NF-κB inhibition is generally considered to be anti-inflammatory, several prior studies have indicated that NF-κB inhibition can have paradoxical effects. As first reported by Lawrence *et al.* (41) in 2001, inhibition of NF-κB during the resolution phase of inflammation can lead to a protracted inflammatory response with prevention of leukocyte apoptosis. More recently, it has been shown that genetic or prolonged pharmacological inhibition of IKKβ in myeloid cells enhances pro-IL-1β processing, leading to increased IL-1β production, increased neutrophilia and increased mortality after endotoxin treatment (32). Although our studies suggest a protective role for the NF-κB pathway in macrophages against tumor promotion and growth, other studies have found that mice with myeloid specific deficiency of IKKβ have reduced tumor number and size (14,42). Indeed, IKKβ deficiency in tumor-associated macrophages can enhance their cytotoxic properties (43,44). These different results may be reconciled by differences in the mouse models employed (i.e. acute versus chronic and tumor transplant versus carcinogenesis models) by the multifaceted composition of the NF-κB pathway (i.e. different components of the pathway may exert divergent functions) and by differences in organ/tissue-specific polarization and function of macrophages. Despite the contradictory literature, our results suggest dual and opposing actions of NF-κB in the lungs: in benign and malignant epithelial cells, NF-κB functions to escalate inflammation and augment carcinogenesis (12,14,15,26,45), whereas activation of the transcription factor in myeloid cells may result in limitation of inflammation and antitumor gate keeping (41,43,46).

The shortcomings of the present work are not to be overlooked. First, the dosing of bortezomib used (1 mg/kg) was likely not relevant to human dosing (~0.03 mg/kg). Second, the carcinogen employed (urethane) is not a prominent carcinogen leading to lung cancer in humans. Third, bortezomib is a proteasome inhibitor and not a specific

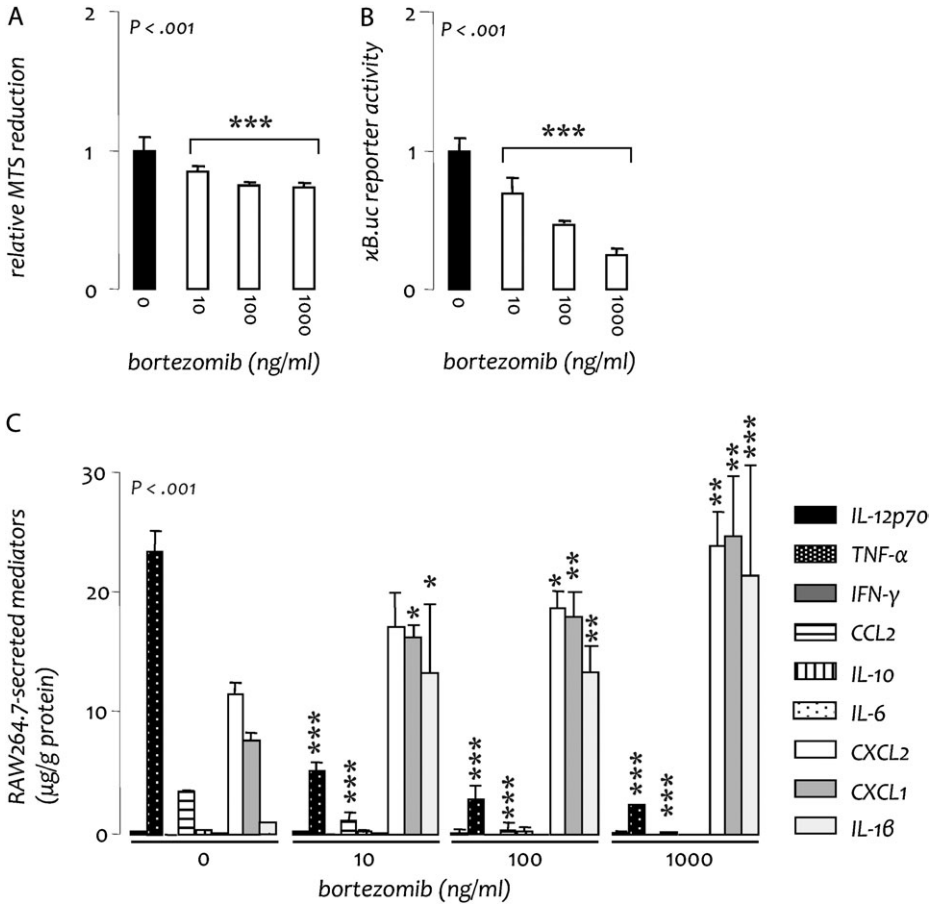

Fig. 6. Bortezomib skews the phenotype of RAW264.7 mouse macrophages *in vitro*. Wild-type and NF-κB reporter (pNGL) RAW264.7 cells were cultured with varying concentrations of bortezomib. (**A**) Cellular proliferation of wild-type cells at 48 h. (**B**) NF-κB-dependent luciferase activity of pNGL cells at 4 h. (**C**) Inflammatory mediator expression at 48 h. All experiments were done thrice; $n = 3$, independent observations for all experiments. IL, interleukin; TNF, tumor necrosis factor; IFN, interferon; *n*, sample size; *P*, probability. Columns, mean; bars, SD. *, ** and ***: $P < 0.05$, 0.01 and 0.001, respectively, compared with bortezomib 0 ng/ml (no treatment).

NF-κB inhibitor; we did not evaluate proteasome inhibition in our models and there is little evidence that the predominant effect of bortezomib is through NF-κB inhibition. The above limit the application of the findings of our study to human lung cancer therapy and chemoprevention. However, our data may prompt further study of the interaction between bortezomib and human lung carcinogens, hopefully validating our results and leading to conclusions pertinent to tailoring human lung cancer chemoprevention strategies.

In conclusion, we inadvertently discovered a tumor-promoting effect of the clinical proteasome inhibitor bortezomib when given in prolonged courses during chemical-induced lung carcinogenesis. The pro-tumorigenic effects of the drug were linked with perpetuation and dysregulation of carcinogen-induced inflammation despite effective blockade of NF-κB activity in both lung epithelial and myeloid cells. Our findings warrant caution when prolonged treatment with bortezomib is contemplated for patients at increased risk for lung cancer.

Funding

This work was supported by a Hellenic Thoracic Society Research grant (to S.P.K. and G.T.S.), by the 'Thorax' Foundation, Athens, Greece (to S.P.K., I.K. and G.T.S.), by US National Institutes of Health grant (HL61419 to T.S.B.), a US Department of Veterans Affairs Merit Review grant (to T.S.B.), by a European Research Council Starting Independent Investigator grant under the European Community's Seventh Framework Program (FP7-IDEAS-ERC-StG-2010-260524 to G.T.S.) and by a European Respiratory Society 2009 Maurizio Vignola Award for Innovation in Pneumology (to G.T.S.).

Conflict of Interest Statement: The authors declare no real or perceived conflict of interest.

References

1. Jemal,A. *et al*. (2011) Global cancer statistics. *CA Cancer J. Clin.*, **61**, 69–90.
2. Parkin,D.M. *et al*. (2005) Global cancer statistics, 2002. *CA Cancer J. Clin.*, **55**, 74–108.
3. Alberg,A.J. *et al*. (2007) Epidemiology of lung cancer: aCCP evidence-based clinical practice guidelines (2nd edition). *Chest*, **132**, 29S–55S.
4. Doll,R. *et al*. (1978) Cigarette smoking and bronchial carcinoma: dose and time relationships among regular smokers and lifelong non-smokers. *J. Epidemiol. Commun. Health*, **32**, 303–313.
5. Peto,R. *et al*. (2006) *Mortality from Smoking in Developed Countries 1950–2000*. Oxford University Press, Oxford, UK. www.ctsu.ox.ac.uk/∼tobacco
6. Sun,S. *et al*. (2007) Lung cancer in never smokers—a different disease. *Nat. Rev. Cancer*, **7**, 778–790.
7. Seow,A. *et al*. (2006) Joint effect of asthma/atopy and an IL-6 gene polymorphism on lung cancer risk among lifetime non-smoking Chinese women. *Carcinogenesis*, **27**, 1240–1244.
8. Schottenfeld,D. *et al*. (2006) Chronic inflammation: a common and important factor in the pathogenesis of neoplasia. *CA Cancer J. Clin.*, **56**, 69–83.
9. Houghton,A.M. *et al*. (2008) Common origins of lung cancer and COPD. *Nat. Med.*, **14**, 1023–1024.
10. Henschke,C.I. *et al*. (2006) Survival of patients with stage I lung cancer detected on CT screening. *N. Engl. J. Med.*, **355**, 1763–1771.
11. Chaturvedi,A.K. *et al*. (2010) C-reactive protein and risk of lung cancer. *J. Clin. Oncol.*, **28**, 2719–2726.

12. Stathopoulos,G.T. *et al*. (2007) Epithelial nuclear factor-κB activation promotes urethane-induced lung carcinogenesis. *Proc. Natl Acad. Sci. USA*, **104**, 18514–18519.
13. Meylan,E. *et al*. (2009) Requirement for NF-kappaB signalling in a mouse model of lung adenocarcinoma. *Nature*, **462**, 104–107.
14. Takahashi,H. *et al*. (2010) Tobacco smoke promotes lung tumorigenesis by triggering IKKbeta- and JNK1-dependent inflammation. *Cancer Cell*, **17**, 89–97.
15. Zaynagetdinov,R. *et al*. (2011) Epithelial nuclear factor-jB signaling promotes lung carcinogenesis via recruitment of regulatory T lymphocytes. *Oncogene,* 2011 Oct 17. doi: 10.1038/onc.2011.480. [Epub ahead of print].
16. Wong,K.K. *et al*. (2010) NF-kappaB fans the flames of lung carcinogenesis. *Cancer Prev. Res. (Phila)*, **3**, 403–405.
17. Inayama,M. *et al*. (2006) A novel IκB kinase-β inhibitor ameliorates bleomycin-induced pulmonary fibrosis in mice. *Am. J. Respir. Crit. Care Med.*, **173**, 1016–1022.
18. LeBlanc,R. *et al*. (2002) Proteasome inhibitor PS-341 inhibits human myeloma cell growth *in vivo* and prolongs survival in a murine model. *Cancer Res.*, **62**, 4996–5000.
19. Richardson,P.G. *et al*. (2003) A phase 2 study of bortezomib in relapsed, refractory myeloma. *N. Engl. J. Med.*, **348**, 2609–2617.
20. Amiri,K.I. *et al*. (2004) Augmenting chemosensitivity of malignant melanoma tumors via proteasome inhibition: implication for bortezomib (VELCADE, PS-341) as a therapeutic agent for malignant melanoma. *Cancer Res.*, **64**, 4912–4918.
21. Rajkumar,S.V. *et al*. (2005) Proteasome inhibition as a novel therapeutic target in human cancer. *J. Clin. Oncol.*, **23**, 630–639.
22. Tang,X. *et al*. (2006) Nuclear factor-kappaB (NF-kappaB) is frequently expressed in lung cancer and preneoplastic lesions. *Cancer*, **107**, 2637–2646.
23. Psallidas,I. *et al*. (2010) Specific effects of bortezomib against experimental malignant pleural effusion: a preclinical study. *Mol. Cancer*, **9**, 56.
24. Fanucchi,M.P. *et al*. (2006) Randomized phase II study of bortezomib alone and bortezomib in combination with docetaxel in previously treated advanced non-small cell lung cancer. *J. Clin. Oncol.*, **24**, 5025–5033.
25. Davies,A.M. *et al*. (2009) Bortezomib plus gemcitabine/carboplatin as first-line treatment of advanced non-small cell lung cancer: a phase II Southwest Oncology Group Study (S0339). *J. Thorac. Oncol.*, **4**, 87–92.
26. Everhart,M.B. *et al*. (2006) Duration and intensity of NF-kappaB activity determine the severity of endotoxin-induced acute lung injury. *J. Immunol.*, **176**, 4995–5005.
27. Nikitin,A.Y. *et al*. (2004) Classification of proliferative pulmonary lesions of the mouse: recommendations of the mouse models of human cancers consortium. *Cancer Res.*, **64**, 2307–2316.
28. Stathopoulos,G.T. *et al*. (2008) Zoledronic acid is effective against experimental malignant pleural effusion. *Am. J. Respir. Crit. Care Med.*, **178**, 50–59.
29. Stathopoulos,G.T. *et al*. (2007) Tumor necrosis factor-α promotes malignant pleural effusion. *Cancer Res.*, **67**, 9825–9834.
30. Stathopoulos,G.T. *et al*. (2006) Nuclear factor-κB affects tumor progression in a mouse model of malignant pleural effusion. *Am. J. Respir. Cell Mol. Biol.*, **34**, 142–150.
31. Stathopoulos,G.T. *et al*. (2008) A central role for tumor-derived monocyte chemoattractant protein-1 in malignant pleural effusion. *J. Natl Cancer Inst.*, **100**, 1464–1476.
32. Greten,F.R. *et al*. (2007) NF-κb is a negative regulator of IL-1β secretion as revealed by genetic and pharmacological inhibition of IKKβ. *Cell*, **130**, 918–931.
33. Di Stefano,A. *et al*. (2002) Increased expression of nuclear factor-kappaB in bronchial biopsies from smokers and patients with COPD. *Eur. Respir. J.*, **20**, 556–563.
34. Caramori,G. *et al*. (2003) Nuclear localisation of p65 in sputum macrophages but not in sputum neutrophils during COPD exacerbations. *Thorax*, **58**, 348–351.
35. Stathopoulos,G.T. *et al*. (2008) Host nuclear factor-kappaB activation potentiates lung cancer metastasis. *Mol. Cancer Res.*, **6**, 364–371.
36. Xue,W. *et al*. (2011) Response and resistance to NF-κB inhibitors in mouse models of lung adenocarcinoma. *Cancer Discov.*, **1**, 236–247.
37. Du,J. *et al*. (2011) Polymorphisms of nuclear factor-{kappa}B family genes are associated with development of multiple myeloma and treatment outcome in patients receiving bortezomib-based regimens. *Haematologica*, **96**, 729–737.
38. Miyakoshi,S. *et al*. (2006) Severe pulmonary complications in Japanese patients after bortezomib treatment for refractory multiple myeloma. *Blood*, **107**, 3492–3494.
39. Thiberville,L. *et al*. (2009) Human *in vivo* fluorescence microimaging of the alveolar ducts and sacs during bronchoscopy. *Eur. Respir. J.*, **33**, 974–985.
40. Rabe,K.F. *et al*. (2007) Global strategy for the diagnosis, management, and prevention of chronic obstructive pulmonary disease: GOLD executive summary. *Am. J. Respir. Crit. Care Med.*, **176**, 532–555.
41. Lawrence,T. *et al*. (2001) Possible new role for NF-kappaB in the resolution of inflammation. *Nat. Med.*, **7**, 1291–1297.
42. Greten,F.R. *et al*. (2004) IKKbeta links inflammation and tumorigenesis in a mouse model of colitis-associated cancer. *Cell*, **118**, 285–296.
43. Fong,C.H. *et al*. (2008) An antiinflammatory role for IKKbeta through the inhibition of ''classical'' macrophage activation. *J. Exp. Med.*, **205**, 1269–1276.
44. Hagemann,T. *et al*. (2008) ''Re-educating'' tumor-associated macrophages by targeting NF-kappaB. *J. Exp. Med.*, **205**, 1261–1268.
45. Cheng,D.S. *et al*. (2007) Airway epithelium controls lung inflammation and injury through the NF-kappa B pathway. *J. Immunol.*, **178**, 6504–6513.
46. Han,W. *et al*. (2009) Myeloid cells control termination of lung inflammation through the NF-{kappa}B pathway. *Am. J. Physiol. Lung Cell. Mol. Physiol.*, **296**, L320–L327.

Received September 7, 2011; revised November 16, 2011; accepted January 21, 2012